

XPS, AES and SEM analysis of recent dental implants

Byung-Soo Kang^{a,*}, Young-Taeg Sul^a, Se-Jung Oh^b, Hyun-Ju Lee^c, Tomas Albrektsson^a

^a Department of Biomaterials/Handicap Research, Institute for Clinical Sciences, The Sahlgrenska Academy at Gothenburg University, Box 412, SE 405 30, Gothenburg, Sweden

^b Department of Physics and Astronomy, Seoul National University, Seoul, South Korea

^c National Center for Inter-University Research Facility, Seoul National University, Seoul, South Korea

Received 19 September 2008; received in revised form 29 December 2008; accepted 26 January 2009

Available online 7 February 2009

Abstract

Today, surface chemistry modifications of titanium implants have become a development strategy for dental implants. The present study investigated the chemistry and morphology of commercially available dental implants (Nobel biocare TiUnite, Astra AB OsseoSpeed, 3i Osseotite, ITI-SLA). X-ray photoelectron spectroscopy (XPS) and auger electron spectroscopy were employed for the analysis of surface chemistry. The morphology was investigated by scanning electron microscopy. The present study demonstrated the major differences of surface properties, mainly dependent on the surface treatment used. The blasting and acid etching technique for the OsseoSpeed, Osseotite and SLA surfaces generally showed mainly TiO₂, but a varying surface morphology. In contrast, the electrochemical oxidation process for TiUnite implants not only produces microporous surface (pore size: 0.5–3.0 μm), but also changes surface chemistry due to incorporation of anions of the used electrolyte. As a result, TiUnite implants contain more than 7 at.% of P in oxide layer and higher amounts of hydroxides compared to the other implants in XPS analysis. F in OsseoSpeed implants was detected at 0.3% before as well as after sputter cleaning.

Crown Copyright © 2009 Published by Elsevier Ltd. on behalf of Acta Materialia Inc. All rights reserved.

Keywords: Clinical dental implants; Surface chemistry; Morphology; X-ray photoelectron spectroscopy (XPS); Titanium

1. Introduction

Surface properties of titanium implants are known as key factors for successful osseointegration [1]. Various surface modification methods have been applied to dental implants in attempts to improve their clinical performance [2–5]. Moreover, the use of updated technologies for implant surface modifications has become a marketing trend in the production of new implants, creating various morphologies as well as surface chemistries. For instance, the electrochemical oxidation process, which has been used on recently launched Mg implant, not only incorporates more than 7 at.% of Mg cations, but also creates a microporous surface [3]. Another new nanoscale process, discrete crystalline deposition, alters surface chemistry as well as

morphology by deposition of 20–100 nm calcium phosphate particles [6]. Hence, detailed surface characterization has become essential for a better understanding of the role of surface properties on implant integration in bone [7–11].

A number of studies have reported the effects of surface chemistry on implant integration in bone [12–14]. Sul and colleagues reported significantly enhanced speed and strength of osseointegration of surface chemistry-modified implants [14–16] and provided experimental indications of a biochemical bonding mechanism on Ca- or Mg-incorporated implants.

The aim of the present study is to investigate the surface chemistry and morphology of recently developed commercially available dental implants (TiUnite[®], OsseoSpeed[®], Osseotite[®], and SLA[®]). These implants are fabricated by proprietary and specific methods which not only produce their original morphology, but also possibly change surface chemistry due to chemical etching or electrochemical

* Corresponding author. Tel.: +46 31 786 2975; fax: +46 31 786 2941.
E-mail address: byung-soo.kang@biomaterials.gu.se (B.-S. Kang).

oxidation [8,17,18]. X-ray photoelectron spectroscopy (XPS) and auger electron spectroscopy (AES) measurements were performed for surface chemistry analyses and depth profile of characteristic elements of the implants, and scanning electron microscopy (SEM) was used for morphological description.

2. Materials and methods

2.1. Implants

TiUnite® (3.75 × 7 mm, Nobel Biocare, Göteborg, Sweden), OsseoSpeed® (4.00 × 11 mm, Astra Tech AB, Möln-

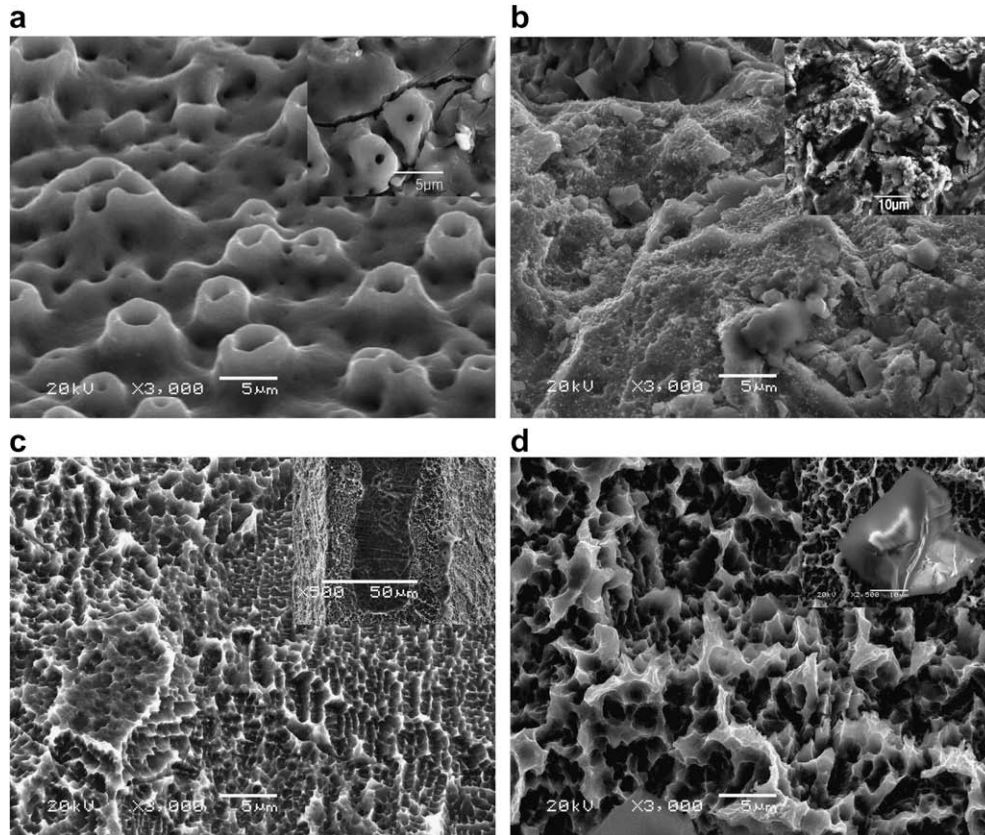


Fig. 1. SEM pictures of clinical implants (3000×): (a) TiUnite; (b) OsseoSpeed; (c) Osseotite; (d) SLA. The inset images in (a), (b), (c) and (d) show crack propagation and oxide particles of TiUnite, deep pits of OsseoSpeed, poorly etched areas of Osseotite and blasting particles of SLA, respectively.

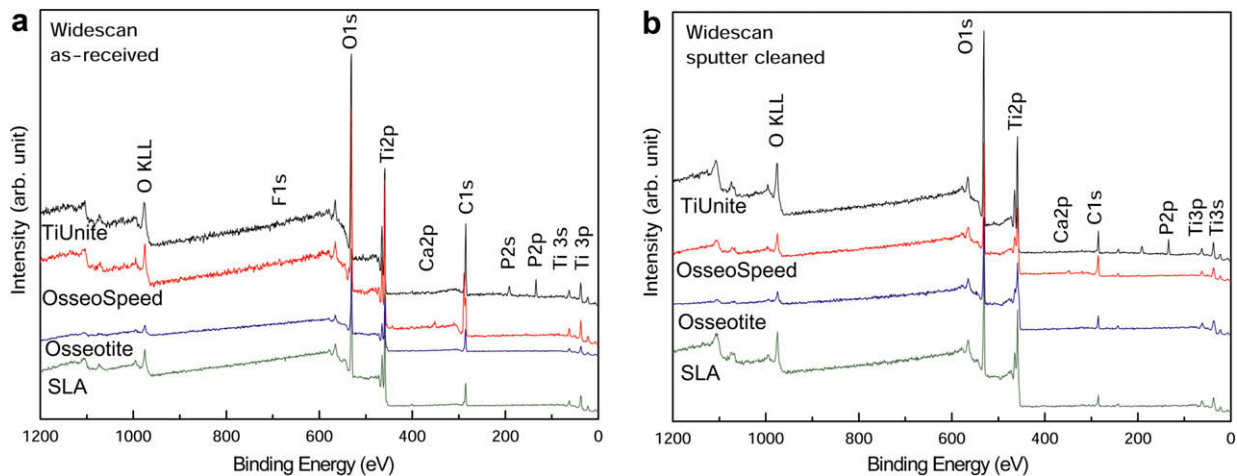


Fig. 2. Survey XPS spectra: (a) XPS spectra of the as-received surfaces; (b) XPS spectra of the sputter-cleaned surfaces. In the case of Osseotite implants, data were acquired from the etched threads.

dal, Sweden), SLA[®] (4.10 × 10 mm, Institute Straumann, Waldenburg, Switzerland), and Osseotite[®] (3.75 × 8.5 mm, Implant Innovation, FL, USA) were purchased from local distributors. Two specimens for each type implant were analyzed by the same protocol of instrumentation described below.

2.2. SEM analysis

SEM (JEOL, LV-6380, Sweden) was used for morphological analysis. The SE mode with an acceleration voltage of 20 kV was selected for SEM analysis and the vacuum pressure was maintained below 1×10^{-5} torr. The load current (LC) was approximately 85 μ A. In order to reflect overall surface morphology, SEM images were acquired at thread flanks of the implants except for SLA. In the case of SLA, images were collected from a screw valley. For the direct comparison of the surface morphology, the same magnification of 3000 \times was selected for all the implants.

2.3. XPS and AES analyses

Surface chemistry was analyzed by XPS (Sigma Probe, Thermo-VG, UK) with monochromatic Al K α (1486.7 eV) X-ray source and a beam size of 400 μ m diameter. X-rays were irradiated on the area between the second and third thread of the implants. The electron take-off angle was fixed at 45° and the vacuum pressure was below 10^{-9} torr during spectra data acquisition. Survey XPS data were acquired over 1200 eV with pass energy of 50 eV and a resolution of 1 eV. XPS spectra were obtained at C 1s, Ti 2p, O 1s, F 1s, P 2p, N 1s, S 2p, Cl 2s and Ca 2p. The operation conditions were over 15–20 eV ranges, pass energy of 20 eV and a resolution of 0.1 eV. XPS data were acquired before and after sputtering. Ar sputter cleaning was operated for 3 s (beam energy = 2 keV, primary current = 2 μ A, rastered area 3.14 mm²). Binding energies, peak areas and atom concentration ratios were obtained using the curve fitting program provided by Product Company (Sigma Probe, Thermo-VG, UK). The binding energy of the photoelectron was refer-

enced to the C (1s) line of adventitious hydrocarbon at 284.8 eV [19].

The depth profiles of chemical composition were measured by AES (Physical Electronics, model PHI 650). The electron beam with 2.5 μ m × 4.0 μ m probing area was accelerated by a 5 kV of acceleration voltage with continuous Ar ions etching of 2 keV at the low 10^{-9} torr (etching rate for amorphous titanium oxide: 3.7 nm min⁻¹).

3. Results

3.1. SEM analysis

Fig. 1a–d revealed characteristic differences at the microlevel according to the surface modification methods used for the implant samples. TiUnite implants showed a porous structure induced by breakdown phenomena during anodic oxidation. Pore size was 0.5–3.0 μ m, sometimes elongated to 10 μ m. The morphology of OsseoSpeed implant was mainly characterized with facets produced by blasting and fine etching pits. The acid-etched surfaces of both Osseotite and SLA implants were similarly characterized by crystallographically oriented boundaries. However, the differences were a needle-like elevation structure with pore sizes of about 1–2 μ m for Osseotite and a honeycomb structure of about 1–3 μ m for SLA implants. Sometimes crack propagation and oxide particles were observed for TiUnite, deep pits for OsseoSpeed, some poorly etched areas at thread peaks of Osseotite and remnants of blasting particles for SLA implants.

3.2. XPS analysis

The survey spectra of as-received and sputter-cleaned surfaces showed major peaks at Ti 2p, O 1s and C 1s (Fig. 2). The peak intensities after sputter cleaning increased at Ti and decreased at C. Relative atom concentrations (at.%) and binding energies of all elements are summarized in Table 1. High-resolution spectra of Ti, O, C, P and F are presented in Fig. 3. The spectra of Ti 2p,

Table 1
Binding energies and atom concentration rate (at.%) of elements at as-received and sputter cleaned implants in XPS analysis.

Element	TiUnite				OsseoSpeed				Osseotite				SLA			
	AR*		SC**		AR		SC		AR		SC		AR		SC	
	at.%	BE	at.%	BE	at.%	BE	at.%	BE	at.%	BE	at.%	BE	at.%	BE	at.%	BE
Ti	12.0	459.0	17.5	459.2	11.8	458.8	20.7	458.8	16.7	458.6	30.9	458.7	20.1	458.7	29.5	458.7
O	45.2	530.7	55.1	530.9	33.1	530.1	39.6	530.3	38.7	530.0	48.4	530.4	47.1	530.1	55.9	530.4
P	6.8	133.4	9.5	133.5	–	–	–	–	–	–	–	–	–	–	–	–
F	–	–	–	–	0.3	684.7	0.4	684.8	–	–	–	–	–	–	–	–
C	35.1	284.8	17.0	284.8	53.2	284.8	58.2	284.8	44.0	284.8	20.8	32.0	32.0	284.8	13.9	284.9
N	1.0	400.5	0.9	400.6	0.3	400.5	–	–	0.6	400.5	–	1.0	1.0	400.6	0.8	400.5
Ca	–	–	–	–	1.3	350.8	1.1	347.5	–	–	–	–	–	–	–	–

AR*, as-received surface; SC**, sputter-cleaned surface, at.%; atomic concentration; BE, binding energy (eV). Full width at half maximum (KWHM) value of O 1s (eV); 2.3 (TiUnite), 1.4 (OsseoSpeed), 1.3 (Osseotite), 1.3 (SLA) for as-received surface and 2.5, 1.5, 1.9, 1.6 for sputter-cleaned surface.

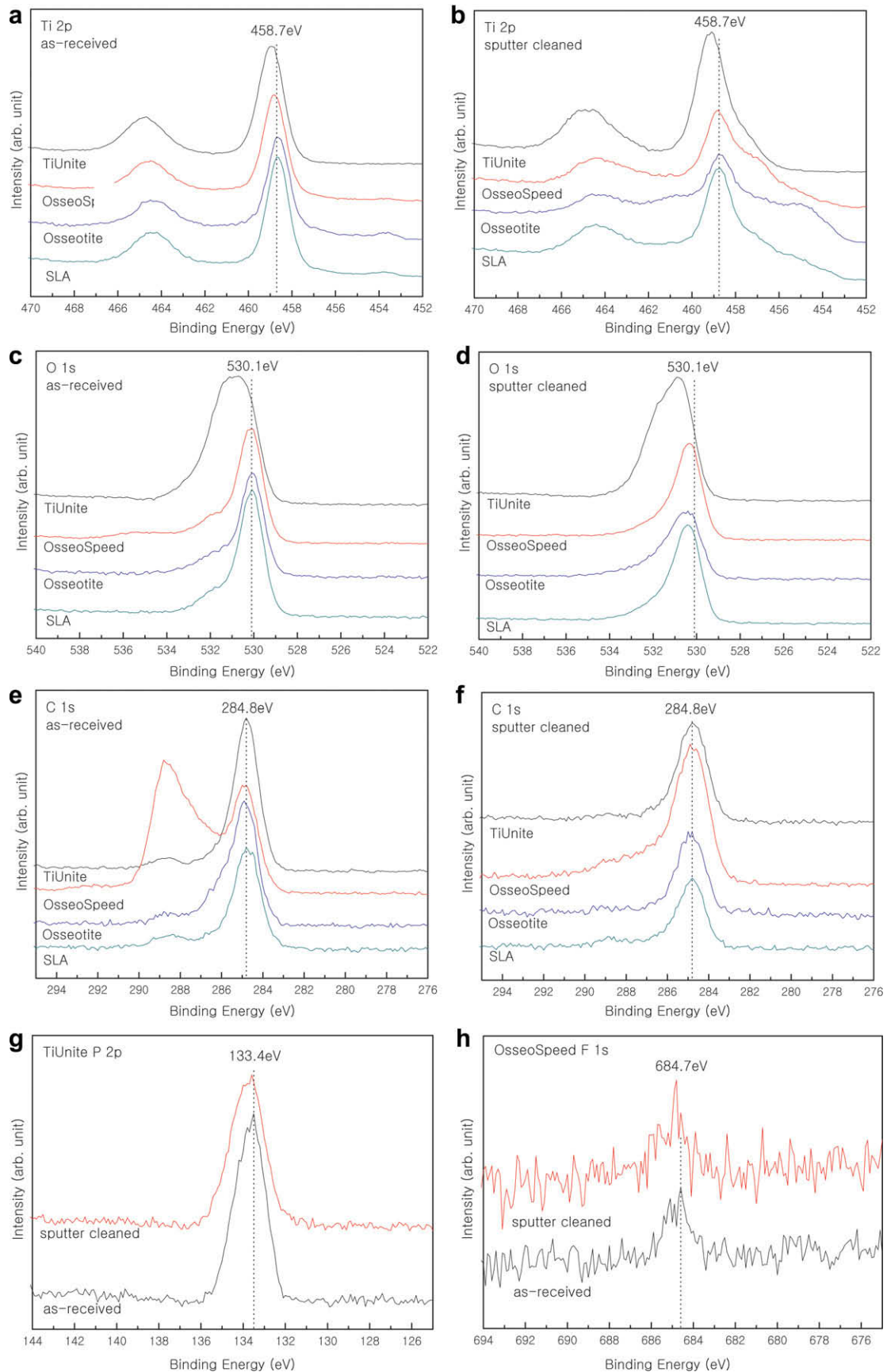


Fig. 3. High-resolution XPS spectra of the as-received and sputter-cleaned samples: (a) and (b) Ti 2p spectra, (c) and (d) O 1s spectra, (e) and (f) C 1s spectra in all the samples; (g) P 2p spectra in TiUnite; (f) F 1s spectra in OsseoSpeed. Dashed lines indicate the binding energy of peak position on the as-received surfaces.

O 1s and C 1s were stoichiometrically deconvoluted (Fig. 4).

The Ti doublet peak, i.e., Ti 2p₁ and Ti 2p₃, of both as-received and cleaned surfaces in Fig. 3a and b appeared near 464.3 eV and 458.7 eV ($\Delta 5.6$ eV) for all the implants except that TiUnite showed a peak intensity at 459.0 eV. After sputter cleaning, binding energy at Ti 2p₃ shifted to high binding energy about 0.2 eV in TiUnite implants but changed negligibly at the other samples. Ti 2p in Fig. 4a were deconvoluted to TiO₂ at 458.7 ± 0.3 eV, hydrated water (Ti–OH) at $\sim 457.9 \pm 0.2$ eV, Ti₂O₃ at $\sim 457.1 \pm 0.3$ eV, TiO at 455.3 ± 0.1 eV and Ti metal at $\sim 454.0 \pm 0.3$ eV.

O 1s spectra of Fig. 3c and d showed main peaks close to 530.1 eV and broadenings at ~ 531.5 and ~ 532.7 eV for OsseoSpeed, Osseotite and SLA implants and at ~ 530.1 – 532 eV for TiUnite implants. The full width at half maxi-

mum (FWHM) of O 1s was greatest for TiUnite implants and showed rather similar features between OsseoSpeed, Osseotite and SLA implants. After sputter cleaning, TiUnite implants showed a sharpened peak of 530.9 eV. In contrast, OsseoSpeed, Osseotite and SLA implants shifted binding energy to the left (~ 0.3 eV) and increased FWHM, i.e., a broadening of the spectra. O 1s spectra in Fig. 4b were deconvoluted to TiO₂, titanium phosphates, (OH)s, C–O, Ti–OH, C=O or C–O, Ti–OH or C=O.

C 1s spectra of Fig. 3e represented a singlet peak at 284.8 eV for TiUnite, Osseotite and SLA implants, while a doublet peak at 284.8 and 288.7 eV was observed for OsseoSpeed implants. Carbon amounts were detected in the range of 32–52 at.%. In particular, OsseoSpeed showed the greatest amount of carbon. In general, the amount of carbon after sputter cleaning was drastically decreased to more or less 20% in TiUnite, Osseotite and SLA implants,

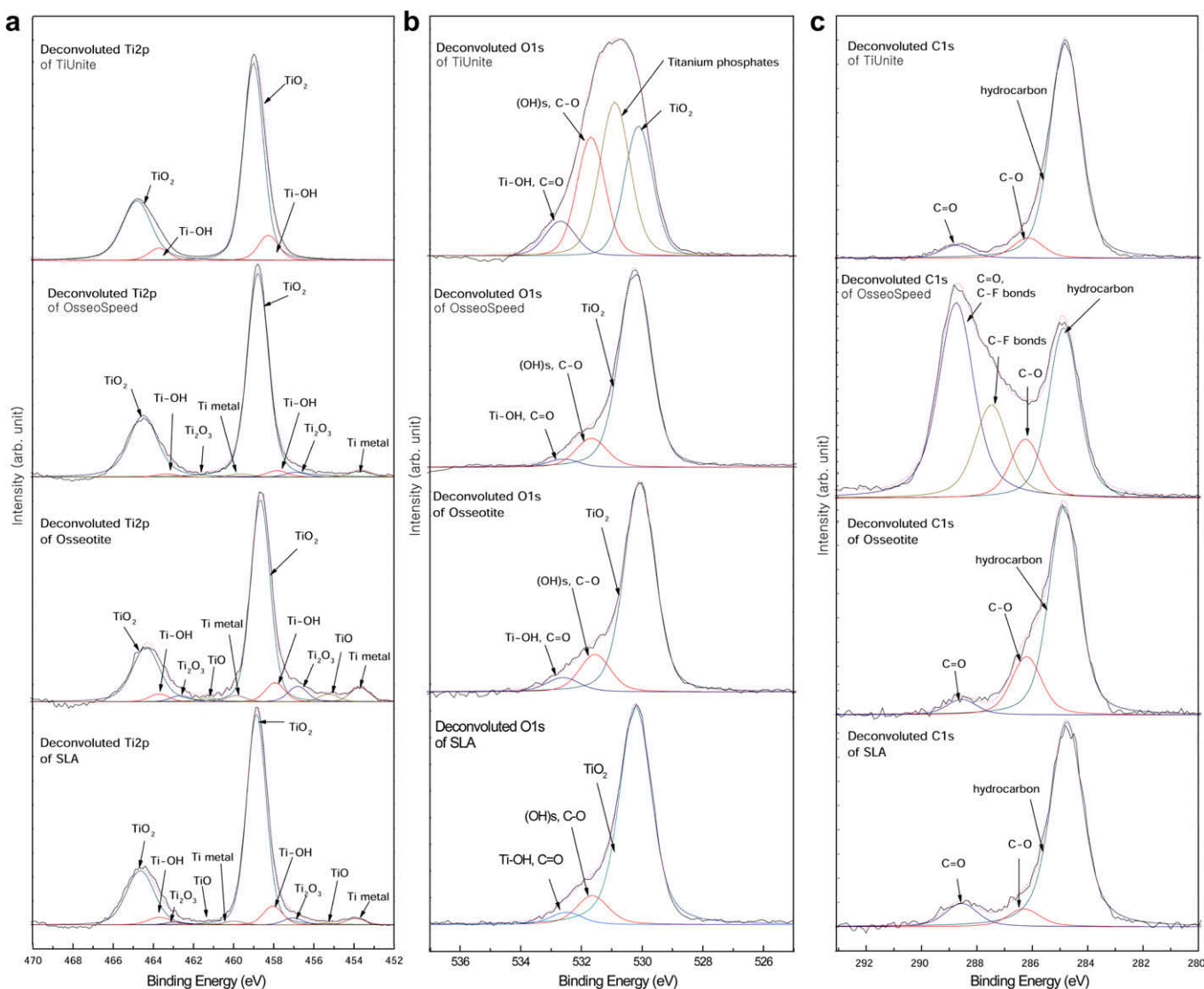


Fig. 4. Deconvoluted XPS data on the as-received surfaces: (a) Ti 2p was fitted to five subpeaks. TiO₂ peak was located at the highest binding energy side, while Ti metal peak was located at the lowest binding energy side; (b) O 1s was fitted to identify the molecular species present. A shoulder to the high binding energy side of the main O 1s peak was composed of (OH)s and Ti–OH; (c) C 1s was fitted with hydrocarbon, C–O, C=O and C–F.

whereas OsseoSpeed implants displayed 38% carbon. However, the C 1s peak at 288.7 eV for OsseoSpeed implants reduced to noise level with an Ar sputtering (Fig. 3f). Deconvolution data of C 1s spectra were imposed to C–O, C–F bonds and C=O (Fig. 4c).

P in TiUnite was detected about 7% at ~133.4 eV (Fig. 3g). After sputtering, the P amount increased to 10%. F in OsseoSpeed was barely detected at 0.3% before and after sputter cleaning (Fig. 3h). N was detected at 0.3–1.2% for all the samples, while Ca was detected in OsseoSpeed at 1.3% for the as-received implants. After sputter cleaning, concentrations of both N and Ca decreased to less than 1.0%. S or Cl were not detected in the samples.

3.3. AES analysis

Ti, O and C were mainly detected in all the implants (Fig. 5). Like the XPS data, the AES analysis confirmed XPS data in that the greatest amount of carbon was found in OsseoSpeed implants and that the amount of F at OsseoSpeed surface was barely detected (Table 2).

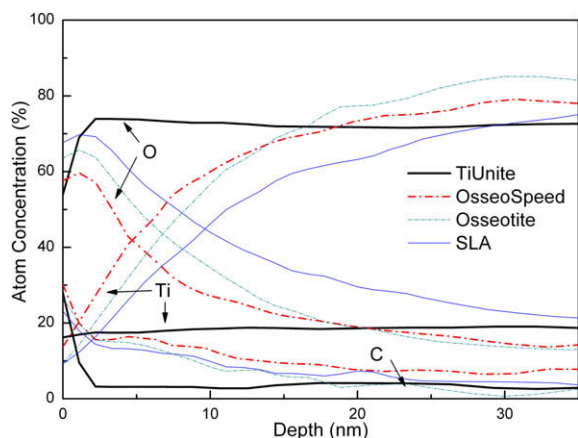


Fig. 5. Element distribution with respect to sputter time of 9 min: Ti, O and C distribution of all implants. AES spectra were acquired at the cutting edge part of the implant samples except for SLA implants. In case of SLA data were collected from a valley of screw.

4. Discussion

The present results showed that surface chemistry and morphology of different commercially available clinical titanium implants differed due to surface modification techniques used during manufacture. As a whole, the blasting and acid etching techniques used for the OsseoSpeed, Osseotite and SLA implants resulted in mainly TiO₂ but rather altered surface morphologies. In contrast, the electrochemical oxidation process for TiUnite implants changed not only surface chemistry due to incorporation of anions of the used electrolyte [15], but also produced a porous structure of the thick oxide layer.

Previous studies on the surface chemistry of machined, turned and blasted implants have reported Ti, O and C as major elements [20–24]. The chemistry-modified implants have revealed more complicated compositions, involving Ca, P, Mg, S, F and Na in association with the used methods [14–16,18,24]. The surface elements of the clinical implants in the present study mainly consisted of Ti, O and C. In addition to TiO₂, nonstoichiometry such as Ti₂O₃ and TiO were also detected. Ti metal peaks were observed at OsseoSpeed, Osseotite and SLA implants, indicating that they have a thin oxide layer. The differences of the binding energy between Ti 2p and O 1s in the present study were consistent with previous studies [22–25].

Most of carbon species exist as surface contaminants since they were abruptly decreased after Ar sputtering. Deconvolution data showed the presence of C–O, C=O and hydrocarbon for all the implants [21]. However, with the highest amounts at 288.7 eV for OsseoSpeed surfaces, a possible explanation for this is the strong electronegativity of F [26]. Previous studies have shown that F concentrations of the implant surfaces vary from 0.6% to 12% [14,24,27,28].

The binding energy of P in TiUnite implant may indicate the presence of titanium phosphates [29]. For this reason, Ti 2p and O 1s of both the as-received and cleaned TiUnite surfaces showed the chemical shifts in the direction of high binding energy as compared to the other implants. AES depth profiles of TiUnite implants support distribution of P in the oxide layer.

Table 2

Atom concentration rate (at%) of elements at as-received and sputter cleaned implants in AES analysis.

Element	TiUnite		OsseoSpeed		Osseotite		SLA	
	AR*	SC**	AR	SC	AR	SC	AR	SC
Ti	16.2	17.5	13.7	34.2	9.4	26.2	9.2	21.1
O	53.9	73.9	55.7	50.2	63.5	58.7	67.7	65.6
P	1.9	5.5	–	–	–	–	–	–
F	–	–	0.4	–	–	–	–	–
C	28.0	3.1	30.2	15.6	26.8	15.1	23.1	13.3
N	–	–	–	–	–	–	–	–
Ca	–	–	–	–	–	–	–	–

AR*, as-received surface; SC**, sputter-cleaned surface. Sputtering time was 54 s. N was not quantitatively evaluated due to the overlap with Ti signal at 390 eV.

Hydrated water (Ti—OH) and hydroxides (OH) were obtained by deconvolution of Ti 2p and O 1s [30,31]. The atom concentration of hydroxides was obviously higher for TiUnite compared to OsseoSpeed, Osseotite and SLA implants. This may be due to an anodic reaction, e.g., $\text{Ti}^{4+}(\text{ox}) + 4\text{H}_2\text{O}(\text{aq}) \rightarrow \text{Ti}(\text{OH})_4(\text{ox}) + 2\text{H}_2 \rightarrow \text{TiO}_{2-x}(\text{OH})_{2x} + (2-x)\text{H}_2\text{O}$ [32]. A large amount of hydroxide and hydrated water in TiUnite contributed to a broad O 1s at high binding energy side. It is generally known that OH groups contribute to the surface hydrophilicity [33].

The binding energy of trace N may be associated to the organic amines [21]. The differences of the relative atom concentration in Tables 1 and 2 may be due to the sensitivity factor to elements of XPS and AES analysis.

A number of in vivo studies have reported that the surface chemistry of titanium implants plays an important role for osseointegration [3,7,12–16,34–36].

Overall, morphology of TiUnite was characterized as a porous structure with a lot of craters created during the breakdown phenomenon of anodic oxidation while the other implants contained etching pits or blasted facets. Fine differences of the pits and facets were obvious between OsseoSpeed, Osseotite and SLA implants due to differences of used blasting and etching parameters [8,17,37]. The mechanism of crack propagation and therefore oxide particle formation in TiUnite is beyond the scope of this study. Blasting particles were detected in SLA implants in all four samples measured. These particles are deemed to be alumina residuals from the blasting process, which was confirmed with EDX analysis [23].

5. Conclusions

The present study demonstrated major differences of the surface properties, according to the surface treatment used, i.e., electrochemical oxidation for the TiUnite implants and a combination of blasting and acid etching technique for the OsseoSpeed, Osseotite and SLA implants. The blasting and acid etching techniques generally do not change the surface elements of the titanium, consisting mainly of TiO_2 , but rather alter the surface morphology. In contrast, the electrochemical oxidation process not only changes surface chemistry due to incorporation of anions from the used electrolytes, but also produced microporous surfaces. In addition to titanium oxide surface chemistry for all the samples, the surface chemistry of TiUnite is characterized by P incorporation into an anodic titanium oxide layer.

Acknowledgments

This research was supported by the research grants of the Biotechnology development project (2007-04306) from the Ministry of Science and Technology of Korea, the VR Foundation, Hjalmar Svensson Research Foundation and Sylvans Foundation.

References

- [1] Albrektsson T, Branemark PI, Hansson HA, Lindstrom J. Osseointegrated titanium implants. Requirements for ensuring a long-lasting, direct bone-to-implant anchorage in man. *Acta Orthop Scand* 1981;52:155.
- [2] Ellingsen JE. Pre-treatment of titanium implants with fluoride improves their retention in bone. *J Mater Sci Mater Med* 1995;6:749.
- [3] Sul YT, Johansson C, Albrektsson T. Which surface properties enhance bone response to implants? Comparison of oxidized magnesium, TiUnite, and Osseotite implant surfaces. *Int J Prosthodont* 2006;19:319.
- [4] Buser D, Schenk RK, Steinemann S, Fiorellini JP, Fox CH, Stich H. Influence of surface characteristics on bone integration of titanium implants. A histomorphometric study in miniature pigs. *J Biomed Mater Res* 1991;25:889.
- [5] Wennerberg A, Albrektsson T, Andersson B. An animal study of c.p. titanium screws with different surface topographies. *J Mater Sci Mater Med* 1995;6:302.
- [6] Mendes VC, Moineddin R, Davies JE. Discrete calcium phosphate nanocrystalline deposition enhances osteoconduction on titanium-based implant surfaces. *J Biomed Mater Res A* 2008;20, June[Epub ahead of print].
- [7] Sul YT, Johansson C, Byon E, Albrektsson T. The bone response of oxidized bioactive and non-bioactive titanium implants. *Biomaterials* 2005;26:6720.
- [8] Ellingsen JE, Johansson CB, Wennerberg A, Holmen A. Improved retention and bone-to-implant contact with fluoride-modified titanium implants. *Int J Oral Maxillofac Implants* 2004;19:659.
- [9] Buser D, Broggini N, Wieland M, Schenk RK, Denzer AJ, Cochran DL, et al. Enhanced bone apposition to a chemically modified SLA titanium surface. *J Dent Res* 2004;83:529.
- [10] Orsini G, Piattelli M, Scarano A, Petrone G, Kenealy J, Piattelli A, et al. Randomized, controlled histologic and histomorphometric evaluation of implants with nanometer-scale calcium phosphate added to the dual acid-etched surface in the human posterior maxilla. *J Periodontol* 2007;78:209.
- [11] Berglundh T, Abrahamsson I, Albouy JP, Lindhe J. Bone healing at implants with a fluoride-modified surface: an experimental study in dogs. *Clin Oral Implants Res* 2007;18:147.
- [12] Skripitz R, Aspenberg P. Tensile bond between bone and titanium: a reappraisal of osseointegration. *Acta Orthop Scand* 1998;69:315.
- [13] Hanawa T, Kamiura Y, Yamamoto S, Kohgo T, Amemiya A, Ukai H, et al. Early bone formation around calcium-ion-implanted titanium inserted into rat tibia. *J Biomed Mater Res* 1997;36:131.
- [14] Sul YT, Byon ES, Jeong Y. Biomechanical measurements of calcium-incorporated oxidized implants in rabbit bone: effect of calcium surface chemistry of a novel implant. *Clin Implant Dent Relat Res* 2004;6:101.
- [15] Sul YT, Johansson CB, Kang Y, Jeon DG, Albrektsson T. Bone reactions to oxidized titanium implants with electrochemical anion sulphuric acid and phosphoric acid incorporation. *Clin Implant Dent Relat Res* 2002;4:78.
- [16] Sul YT, Johansson C, Chang BS, Byon ES, Jeong Y. Bone tissue responses to Mg-incorporated oxidized implants and machine-turned implants in the rabbit femur. *J Appl Biomater* 2005;3:18.
- [17] Szmukler-Moncler S, Testori T, Bernard JP. Etched implants: a comparative surface analysis of four implant systems. *J Biomed Mater Res B Appl Biomater* 2004;69B:46.
- [18] Hall J, Lausmaa J. Properties of a new porous oxide surface on titanium implants. *Appl Osseointegration Res* 2001;1:5.
- [19] Moulder JF, Sobol PE, Stickle WF. Handbook of X-ray photoelectron spectroscopy: a reference book of standard spectra for identification and interpretation of XPS data. Eden Prairie, MN: Physical Electronics Inc.; 1995.
- [20] Klauber C, Lenz LJ, Henry PJ. Oxide thickness and surface contamination of six endosseous dental implants determined by

- electron spectroscopy for chemical analysis: a preliminary report. *Int J Oral Maxillofac Implants* 1990;5:264.
- [21] Brunette DM. Titanium in medicine: material science, surface science, engineering, biological responses and medical applications. Berlin: Springer; 2001.
- [22] Sawase T, Hai K, Yoshida K, Baba K, Hatada R, Atsuta M. Spectroscopic studies of three osseointegrated implants. *J Dent* 1998;26:119.
- [23] Massaro C, Rotolo P, De Riccardis F, Milella E, Napoli A, Wieland M, et al. Comparative investigation of the surface properties of commercial titanium dental implants. Part I. Chemical composition. *J Mater Sci Mater Med* 2002;13:535.
- [24] Olefjord I, Hansson S. Surface analysis of four dental implant systems. *Int J Oral Maxillofac Implants* 1993;8:32.
- [25] Lausmaa J. Surface spectroscopic characterization of titanium implant materials. *J Electron Spectrosc Related Phenomena* 1996;81:343.
- [26] Nanse G, Papirer E, Fioux P, Moguet F, Tressaud A. Fluorination of carbon blacks: an X-ray photoelectron spectroscopy study. I. A literature review of XPS studies of fluorinated carbons. XPS investigation of some reference compounds. *Carbon* 1997;35:175.
- [27] Nygren H, Eriksson C, Lausmaa J. Adhesion and activation of platelets and polymorphonuclear granulocyte cells at TiO₂ surfaces. *J Lab Clin Med* 1997;129:35.
- [28] Morra M, Cassinelli C, Bruzzone G, Carpi A, Di Santi G, Giardino R, et al. Surface chemistry effects of topographic modification of titanium dental implant surfaces. I. Surface analysis. *Int J Oral Maxillofac Implants* 2003;18:40.
- [29] Wang Q, Zhong L, Sun J, Shen J. A Facile layer-by-layer adsorption and reaction method to the preparation of titanium phosphate ultrathin films. *Chem Mater* 2005;17:3563.
- [30] Healy KE, Ducheyne P. Hydration and preferential molecular adsorption on titanium in vitro. *Biomaterials* 1992;13:553.
- [31] Sodhi RNS, Weninger A, Davies JE, Sreenivas K. X-ray photoelectron spectroscopic comparison of sputtered Ti, Ti6Al4V, and passivated bulk metals for use in cell culture techniques. *J Vac Sci Technol A Vac Surf Films* 1991;9:1329.
- [32] Ohtsuka T, Nomura N. The dependence of the optical property of Ti anodic oxide film on its growth rate by ellipsometry. *Corros Sci* 1997;39:1253.
- [33] Sakai N, Wang R, Fujishima A, Watanabe T, Hashimoto K. Effect of ultrasonic treatment on highly hydrophilic TiO₂ surfaces. *Langmuir* 1998;14:5918.
- [34] Sul YT, Jeong Y, Johansson C, Albrektsson T. Oxidized, bioactive implants are rapidly and strongly integrated in bone. Part 1. Experimental implants. *Clin Oral Implants Res* 2006;17:521.
- [35] Virtanen S, Milosev I, Gomez-Barrena E, Trebse R, Salo J, Konttinen YT. Special modes of corrosion under physiological and simulated physiological conditions. *Acta Biomater* 2008;4:468.
- [36] Morais LS, Serra GG, Muller CA, Andrade LR, Palermo EFA, Elias CN, et al. Titanium alloy mini-implants for orthodontic anchorage: immediate loading and metal ion release. *Acta Biomater* 2007;3:331.
- [37] Fandridis J, Papadopoulos T. Surface characterization of three titanium dental implants. *Implant Dent* 2008;17:91.